OPEN

Correspondence and
requests for materials
should be addressed to
A.B.B. (anatoly@kth.
se)

Atomic Diffusion in Solid Molecular Hydrogen

Anatoly B. Belonoshko[1], Muhammad Ramzan[2], Ho-kwang Mao[3,4] & Rajeev Ahuja[2,5]

[1]Condensed Matter Theory, Department of Theoretical Physics, AlbaNova University Center, KTH Royal Institute of Technology, SE-106 91 Stockholm, Sweden, [2]Condensed Matter Theory Group, Department of Physics and Astronomy, Box 516, Uppsala University, SE-751 20, Uppsala, Sweden, [3]Geophysical Laboratory, Carnegie Institution of Washington, Washington DC 20015, USA, [4]Center for High Pressure Science and Technology Advanced Research, 1690 Cailun Rd, bldg 3, 2nd fl, Shanghai 201203, P. R. China, [5]Applied Materials Physics, Department of Materials Science and Engineering, KTH Royal Institute of Technology, SE-100 44 Stockholm, Sweden.

We performed ab initio molecular dynamics simulations of the C2c and Cmca-12 phases of hydrogen at pressures from 210 to 350 GPa. These phases were predicted to be stable at 0 K and pressures above 200 GPa. However, systematic studies of temperature impact on properties of these phases have not been performed so far. Filling this gap, we observed that on temperature increase diffusion sets in the Cmca-12 phase, being absent in C2c. We explored the mechanism of diffusion and computed melting curve of hydrogen at extreme pressures. The results suggest that the recent experiments claiming conductive hydrogen at the pressure around 260 GPa and ambient temperature might be explained by the diffusion. The diffusion might also be the reason for the difference in Raman spectra obtained in recent experiments.

Being the lightest and the most abundant element in the universe, hydrogen is a fascinating substance. The metallization of dense hydrogen has been one of the central topics since the first theoretical prediction of transition to a monatomic metallic state of molecular hydrogen at 25 GPa by Wigner and Huntington in 1935[1]. Since then a series of theoretical and experimental studies have been employed but could not completely unveil the structural and electronic properties of hydrogen at high pressures[2]. Solid hydrogen remains an electrical insulator[3,4] up to the pressure of 342 GPa at temperatures below 100 K. In Ref. 3, hydrogen was observed as a non-metallic up to 320 GPa at 77 K. Metallic monatomic hydrogen has been predicted[5] to exist in the liquid phase at high temperature and pressure. It has been reported that the hydrogen remains molecular up to 285 GPa at T<140 K[6,7]. Pickard and Needs[8] presented the zero temperature phase diagram of solid hydrogen up to ≈400 GPa, predicting the most stable phases remained to be insulating up to 400 GPa.

Recently[9] the metallization of hydrogen at ambient temperature and pressures in the range 260–270 GPa was reported, suggesting the further detailed and comprehensive studies of this element. Other studies suggested that hydrogen remain insulating[10] at the very same conditions and suggested[11] that the experimental data was contaminated due to certain shortcomings of the experimental technique. In such situation theory becomes a useful tool allowing to look at the phenomena possibly causing the disagreement between these observations.

To the best of our knowledge, the x-ray determination of the high pressure structures of solid hydrogen could not be performed by the experiments due to the extremely weak x-ray scattering of hydrogen. Only the experimental findings through Raman and visible transmission spectroscopy[10] are available in the literature. Also, there is a number of theoretical papers that render other phases stable at high-PT[12–16]. The main purpose of the present work, however, is to study the impact of temperature on the structures predicted to be stable at relevant P and zero temperature. Therefore, we have chosen to investigate the C2c and Cmca-12 phases, relevant to the range of pressures in recent experiments. These phases were found stable above 200 GPa by Pickard and Needs[8]. Since the impact of temperature is expected to be critical (no metallization according to Loubeyre et al.[3] at 77 K and metallization according to Eremets and Troyan[9] at 300 K), we employed molecular dynamics (MD) method that allows to account for temperature impact.

Results

We found that the impact of temperature is critical. Hydrogen atoms abruptly become diffusing before melting on temperature increase. Intramolecular bonding becomes rather weak at high pressure[17] that explains easy pairing-depairing process[18]. This might explain the difference between the Loubeyre et al.[3] and Eremets and Troyan[9] experiments. The apparent contradiction between the metallization and no-metallization experiments could be

explained by the evacuation of the hydrogen from the experimental cell in experiments by Eremets and Troyan[9] due to a sudden onset of diffusion on the C2c to Cmca-12 transition.

We note that Howie et al.[10] did not measure conductivity therefore there is no direct controversy between their and Eremets and Troyan[9] experiments. While the claim for metallic hydrogen might be unjustified as argued in Ref. 11, we demonstrate that there is the mechanism that might lead to the drop in resistance at ambient temperature and high pressure. Also, the drop in resistance might be anisotropic.

Hydrogen melts at a much higher temperatures than the ambient temperature in the Eremets and Troyan experiment. The hydrogen melting curve bends down but not fast enough to become liquid at 260 GPa. Our hydrogen melting points at 652 K and 261 GPa and 567 K and 288 GPa are in good agreement with the melting curve depicted in Fig. 1 of Ref. 10 and the melting point very recently calculated by Liu et al.[13]. The diffusive state might be an intermediate between the Cmca-12 and the Ibam structure[10] and/or Cmca-4 structure[13]. It is possible that these structures have actually formed in our MD simulations (Fig. 2).

Discussion

We performed MD simulations (see Methods) for the constant volume starting with the C2c and Cmca-12 (12 atoms in a primitive unit cell) structures. The cell parameters were obtained from relaxation calculations at pressures of 210 GPa, 260 GPa, 305 GPa and 350 GPa, respectively. Then for a number of temperatures we performed MD runs. For each isochore melting point was computed by the Z method[19]. The computed 4 points are shown in Fig. 1 along with the Z-shaped isochores. Pressure drops on melting, indicating negative volume of melting in accordance with previous studies. Our melting curve, computed at $200 < P < 350$ GPa, compares well with available data in literature. In Fig. 1, we have shown our P-T computed points, where the sharp P changes at 852 K, 652 K, 567 K and 482 K, for C2c and Cmca-12 phases, representing the melting transitions at these temperatures.
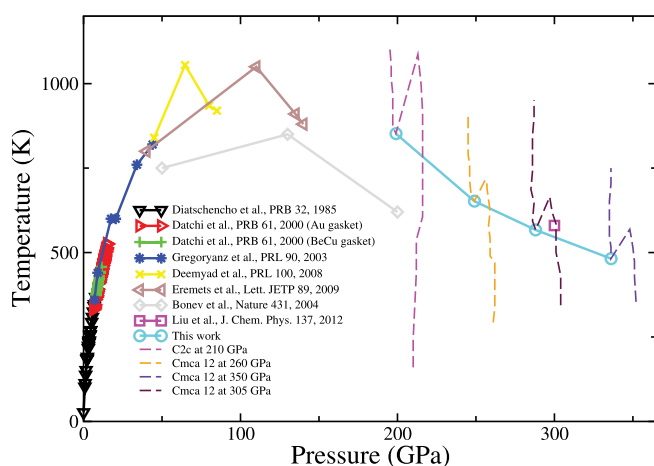

Figure 1 | Melting curve of hydrogen. The circles represent the melting P-T points computed in this study by the Z method[19] (recently confirmed for molecular systems[20]). The sharp P changes at 852 K, 652 K, 567 K and 482 K, for C2c at 210 GPa, Cmca-12 at 260 GPa, Cmca-12 at 305 GPa, and Cmca-12 at 350 GPa respectively. The inverted triangles are experimental points from Diatschenko et al. (Ref. 28), right triangles and pluses are experimental points from Datchi et al. (Ref. 29), the stars are experimental points from Gregoryanz et al. (Ref. 30), the crosses are experimental points from Deemyad et al. (Ref. 31), left triangles are experimental points from Eremets et al. (Ref. 32), the diamonds are ab initio data from Bonev et al. (Ref. 5), and the square is the very recently calculated melting point of hydrogen by Liu et al. (Ref. 13).

Fig. 3 shows mean square displacement for these phases at a number of temperatures as a function of time. In Fig. 3a, we could not see any diffusion for C2c phase and the melting transition occurs at T = 852 K, whereas in Fig. 3b, the significant diffusion can be observed at T = 490 K for Cmca-12 phase. Note that at T > 490 K, the simulated solid state is metastable, because the hydrogen melts at 652 K (see Fig. 3b). The same trend can also be seen for Cmca-12 phases at 305 GPa and 350 GPa (Fig. 3c and 3d respectively, where the diffusion can be seen at T = 501 K and T = 429 K respectively and the melting occurs at T = 567 K and T = 482 K respectively).

Conductive hydrogen was claimed to be observed at 260 GPa. Let us take a closer look at the data for this pressure.

Calculated radial distribution functions for Cmca-12 structure at 260 GPa, at a number of temperatures are shown in Fig. 4 and Fig. 5. One can see that the distance between the central hydrogen atom and the atoms in the first neighbour shell is very short (≈ 1.2 Å). This suggests that at elevated temperature the atoms that belong to different molecules might come closer to each other than to the atoms in their 'native' molecule. That might lead to exchange of the atoms and, thus, to hydrogen diffusion in solid molecular hydrogen. Indeed, on the T increase we observe that the first (molecular) peak of RDF and the second (1st neighbour) peak start overlap (Fig. 4). When the diffusion sets in, the RDF becomes considerable (non-zero) at the distances intermediate between the intramolecular peak at 0.72 Å and intermolecular peak at 1.2 Å (it forms a shoulder rather than a peak at high T; it can be seen as a peak at low T (Fig. 5). This overlap becomes pronounced at temperatures between 400 K and 500 K. We closely monitored the mobility of hydrogen atoms and we observed that at around 490 K the hydrogen atoms depair[18] and create new pairs, facilitating, in this way, diffusion of H atoms. Fig. 3b shows mean square displacement for Cmca-12 phase at 260 GPa, at a number of temperatures as a function of time.

Clearly, there is no diffusion below 490 K. One can see that at all temperatures before onset of melting the hydrogen preserves a layered structure (Fig. 2). The melting was computed by the Z method[19] that was recently demonstrated to perform well for molecular crystals[20]. The melting occurs at 652 K (see inset in Fig. 4) with negative volume change. This suggests that the melting curve of hydrogen has a maximum proposed earlier, however the temperature is still high enough to rule out the Eremets and Troyan[9] explanation of metallization by melting transition. The layered structure of hydrogen suggests that diffusion proceeds through layers. Fig. 2 shows the trajectories of hydrogen atoms in the central layer. We see (Fig. 2) that there is no diffusion up to about 490 K. The atoms are moving with considerable amplitude, yet they stay bonded with the same atom through the whole simulation time. At about 490 K the picture is completely different. The continuous bands or, rather, diffusion channels are formed. The diffusion clearly stays within layers. There is no diffusion along 100 and 010 even at much higher temperature of 657 K.

Thus we observe a temperature induced transition from non-diffusive to the diffusive state in solid molecular hydrogen. In our MD simulations we could not consider zero point motion (ZPM) that is considerable at these pressures. Indeed, the vibron frequency of 4000 cm^{-1} implies the amplitude of ZPM is equal to 0.16 Å. This is equivalent to the amplitude of thermal motion of 200 K (Fig. 4). Therefore, the cumulative impact of thermal and zero point motion might cause the diffusion at already 300 K.

Note, that for deuterium to become diffusive the temperature needs to be higher than for hydrogen. First, the ZPM amplitude for D is smaller (0.1 Å). Second, the amplitude of thermal motion is also smaller at the same temperature. Therefore, exchange of D atoms might require temperatures of 400 K and higher, unlike for H where 300 K seem to be sufficient.

We analyzed the charge that diffusing H atom can carry (Fig. 6). By performing Bader analysis[21,22], we computed charges on H atoms
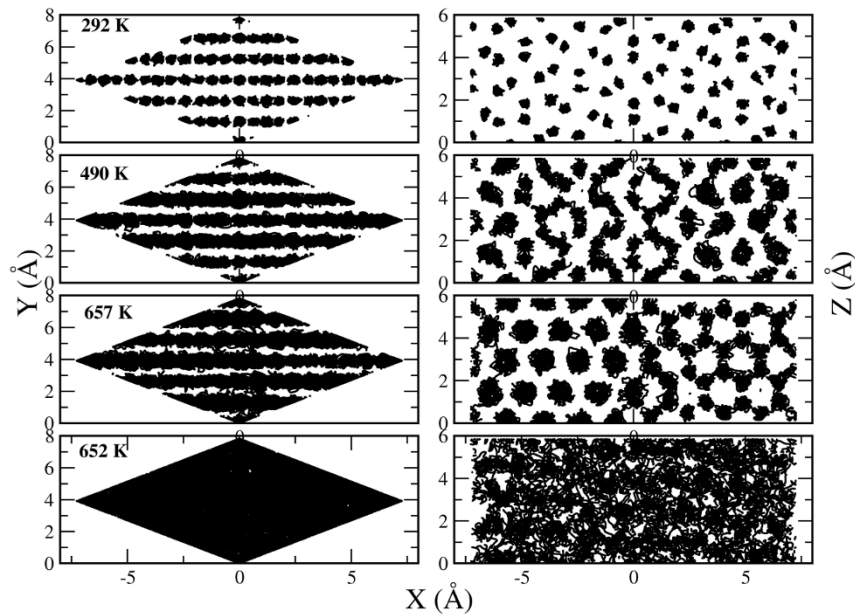
Figure 2 | Trajectories of atoms for Cmca-12 at 260 GPa. The left panels show XY (along Z) projections of all 216 atoms computed at the last 4000 timesteps of MD runs at the temperatures (from top to bottom) 292, 490, 657, and 652 K. All runs show layered structure of hydrogen except the last one which is a liquid structure. The right panels show the XZ projections of the central (the longest) layer in the computational cell for the run on the left. At T = 292 K there is no diffusion, all atomic positions during the run are confined to the close neighborhood of the original crystallographic positions. At T = 490 K one can see formation of connected patterns indicating the ionic diffusion of hydrogens. At T = 657 K this formation is fully developed in the computational cell. At T = 652 K in the liquid state the lattice is gone and the atoms homogeneously fill the cell.
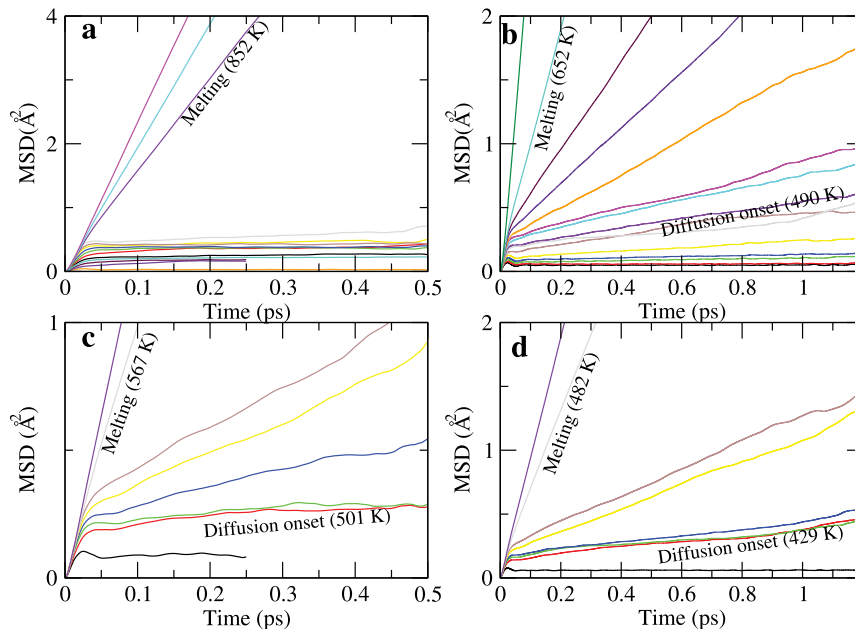

Figure 3 | Hydrogen diffusion. Mean square displacement (MSD) $<(r(t)-r(0))^2>$, where $r(t)$ is the radius vector of the system at the time moment t, is shown for: (a) C2c at 210 GPa: There is no diffusion – the MSD is constant corresponding to quickly reached equilibrium state with the thermal movement around the equilibrium lattice positions up to T < 852 K. At melting temperature 852 K (Fig. 1) the diffusion starts in liquid. (b) Cmca-12 at 260 GPa: computed for the same temperatures as in Fig. 3a and shown by the same colors. At low T there is no diffusion – the MSD is constant corresponding to quickly reached equilibrium state with thermal motion around the equilibrium lattice positions. At T = 490 K the state is different because the diffusion sets in. On the temperature increase, diffusion increases. Diffusion in liquid (T = 652 K) is about order of magnitude larger than diffusion in solid at about the same (T = 657 K) temperature. However, this is a very large diffusion for a solid. The MSD is weakly dependent on T as soon as the diffusion starts in the solid state (490 K < T < 657 K). (c) Cmca-12 at 305 GPa: At low T there is no diffusion – the MSD is constant corresponding to quickly reached equilibrium state with thermal movement around the equilibrium lattice positions. At T = 501 K the state is different because the diffusion sets in. Diffusion increases with temperature. Diffusion in liquid (T = 567 K) is about order of magnitude larger than diffusion in solid at about the same (T = 585 K) temperature. The MSD just slightly dependent on T as soon as the diffusion starts in the solid state (501 K < T < 585 K). (d) Cmca-12 at 350 GPa: At low T there is no diffusion – the MSD is constant corresponding to quickly reached equilibrium state with thermal movement around the equilibrium lattice positions. At T = 429 K the state is different because the diffusion sets in. Diffusion increases with temperature. Diffusion in liquid (T = 482 K) is about order of magnitude larger than diffusion in solid at about the same (T = 473 K) temperature. The MSD just slightly dependent on T as soon as the diffusion starts in the solid state (429 K < T < 473 K).
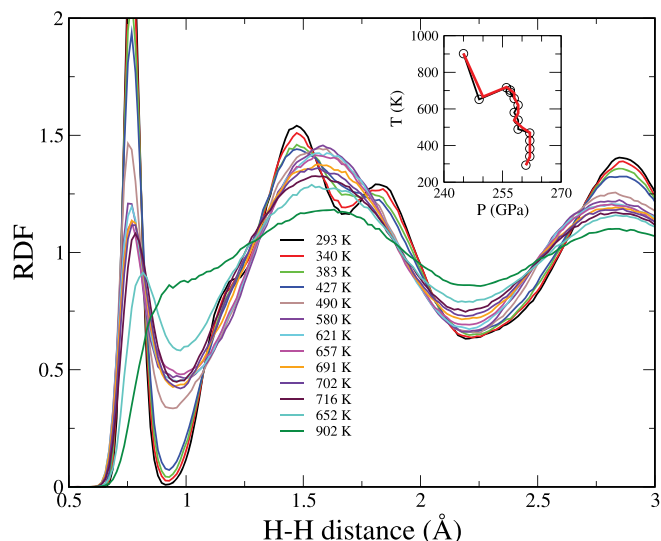
Figure 4 | Radial distribution functions of hydrogen for Cmca-12 and P close to 260 GPa. RDFs are simulated at the density 1.54083 Å³/atom and temperatures as indicated in legend. Corresponding pressure (P) at T = 0 K is equal 259 GPa. The inset shows P-T computed points (the black points are averaged over last 4000 timesteps and the red points are averaged over last 2000 timesteps). The sharp P change at T = 652 K occurs on melting transition. The RDF can be divided in 3 sets. The first set is for T<490 K where the first molecular peak of RDF at r = 0.72 Å and the second peak at r = 1.2 Å are overlapping just slightly. The second set is for 490 K < T < 716 K where significant diffusion is observed (Fig. 3b), Note, that at T> 652 K the simulated solid state is metastable, because the hydrogen melts (see inset) at 652 K. The third set consists of RDFs corresponding to liquid state at 652 K and 902 K. At these temperatures the first peak is not present, which is the evidence for transformation to monatomic liquid.

at a number of temperatures (Fig. 6). One can see that below the diffusion threshold the charge is close to 1 e., interesting that the charge distribution is asymmetric as predicted by Baranowski[23]. The charge distribution becomes much wider in diffusing state and similar to the distribution in the liquid state. Considering that the liquid monatomic state is metallic it is possible that the diffusing state is also
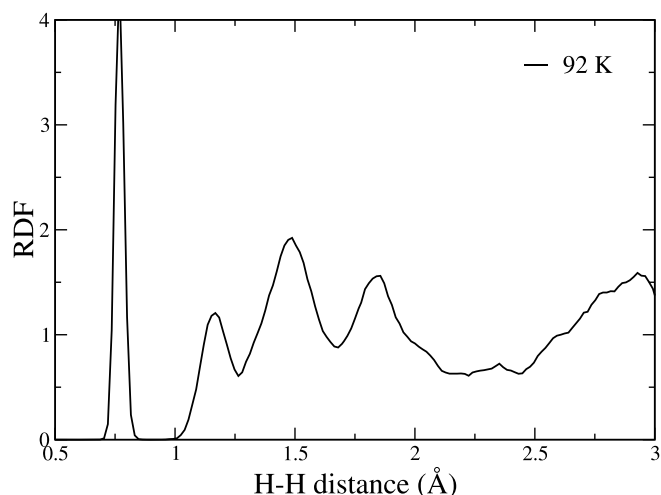

Figure 5 | Radial distribution function (RDF) of hydrogen for Cmca-12 at the density 1.54083 Å³/atom and T = 92 K. Corresponding pressure (P) at T = 0 K is equal 259 GPa. The intermolecular peak at 1.2 Å is clearly seen. The first and second peaks are well separated implying no diffusion. The peak becomes a shoulder at high temperature (Fig. 4).
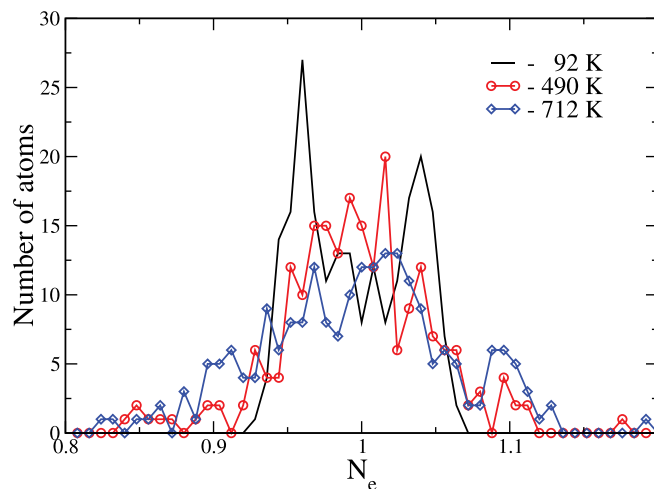

Figure 6 | Density of states for the charge distribution according to Bader procedure for Cmca-12 at 260 GPa. The DOS at 92 K in non-diffusive state is narrow and asymmetric. The DOS in diffusive and liquid states are wide and similar implying similar electronic structure.

conductive. Also, considering that in these experiments hydrogen might recrystallize and that the diffusion proceeds along the 001 direction, different experiments might lead to different observations due to the different grains orientation. The bandgap in our simulations is closing but it is known that DFT normally underestimates bandgaps[24,25].

If we extrapolate our melting curve (Fig. 1), we find the melting points at around 460 GPa at T = 300 K and 540 GPa at T = 0 K. Given that the liquid hydrogen is non-molecular and metallic, this provides us with the upper limit for the onset of metallicity in hydrogen. This is, of course, if other solid-solid transitions will not significantly increase the hydrogen melting temperature.

Methods

We have performed our ab initio molecular dynamics (MD) calculations with the use of Projector Augmented Wave (PAW) method[26], as implemented in the Vienna Ab initio Simulation Package (VASP) code[24,25]. The Perdew, Burke, and Ernzerhof (PBE)[27] variant of the generalized gradient approximation (GGA) was used for the exchange correlation functional. The Gaussian smearing method with a 0.05 eV smearing width was used for the Brillouin zone integration. We have employed $3 \times 3 \times 2$ k-points mesh to sample the Brillouin zone. The energy cutoff was equal to 520 eV. These values were found sufficient to produce converging results. The Verlet algorithm is used to integrate the equation of motion, with a time step of 0.25 fs (1 fs = 10^{-15} s). The duration of each MD run was 10000 time steps. Calculation of intermediate averages showed that this is enough to obtain converging averages (see Fig. 1 and inset in Fig. 4). The initial configuration in every run was fully optimized for C2c and Cmca-12 structures[8] with 216 hydrogen atoms. We have performed a series of simulations in the microcanonical ensemble, with a constant volumes, like 1.5408 Å³/atom (P = 259 GPa at T = 0 K) for one of the studied Cmca-12 structure at 260 GPa, varying initial temperatures[19]. From these simulations, the corresponding melting curve of hydrogen, mean square displacements (MSD's), radial distribution functions (RDF's), trajectories, pressures and temperatures were derived and analyzed.

1. Wigner, E. & Huntington, H. B. On the possibility of a metallic modification of hydrogen. *J. Chem. Phys.* **3**, 764–770 (1935).
2. Mao, H. K. & Hemley, R. J. Ultrahigh pressure transitions in solid hydrogen. *Rev. Mod. Phys.* **66**, 671–692 (1994).
3. Loubeyre, P., Occelli, F. & LeToullec, R. Optical studies of solid hydrogen to 320 GPa and evidence for black hydrogen. *Nature* **416**, 613–617 (2002).
4. Narayana, C., Luo, H., Orloff, J. & Ruoff, A. L. Solid hydrogen at 342 GPa: no evidence for an alkali metal. *Nature* **393**, 46–49 (1998).
5. Bonev, S. A., Schwegler, E., Ogitsu, T. & Galli, G. A quantum fluid of metallic hydrogen suggested by first-principles calculations. *Nature* **431**, 669–672 (2004).
6. Tse, J. S. & Klug, D. D. Evidence from molecular dynamics simulations for non-metallic behavior of solid hydrogen above 160 GPa. *Nature* **378**, 595–597 (1995).
7. Goncharov, A. F., Gregoryanz, E., Hemley, R. J. & Mao, H.-K. Spectroscopic studies of the vibrational and electronic properties of solid hydrogen to 285 GPa. *Proc. Natl. Acad. Sci. USA* **98**, 14234–14237 (2001).

8. Pickard, C. J. & Needs, R. J. Structure of phase III of solid hydrogen. *Nature Physics* **3**, 473–476 (2007).
9. Eremets, M. I. & Troyan, I. A. Conductive dense hydrogen. *Nature Materials* **10**, 927 (2011).
10. Howie, R. T., Guillaume, C. L., Scheler, T., Goncharov, A. F. & Gregoryanz, E. Mixed molecular and atomic phase of dense hydrogen. *Phys. Rev. Lett.* **108**, 125501, 2012.
11. Nellis, W. J., Ruoff, A. L. & Silvera, I. F. Has Metallic Hydrogen Been Made in a Diamond Anvil Cell?. arXiv: 1201.0407.
12. Johnson, K. A. & Ashcroft, N. W. Structure and bandgap closure in dense hydrogen. *Nature* **403**, 632–635 (2000).
13. Liu, H., Zhu, L., Cui, W. & Ma, Y. Room-temperature structures of solid hydrogen at high pressures. *J. Chem. Phys.* **137**, 074501 (2012).
14. Pickard, C. J., Martinez-Canales, M. & Needs, R. J. Density functional theory study of phase IV of solid hydrogen. *Phys. Rev. B* **85**, 214114 (2012).
15. Liu, H., Wang, H. & Ma, Y. Quasi-Molecular and Atomic Phases of Dense Solid Hydrogen. *J. Phys. Chem. C* **116**, 9221–9226 (2012).
16. Liu, H. & Ma, Y. Proton or Deuteron Transfer in Phase IV of Solid Hydrogen and Deuterium. *Phys. Rev. Lett.* **110**, 025903 (2013).
17. Hemley, R. J., Soos, Z. G., Hanfland, M. & Mao, H.-K. Charge-transfer states in dense hydrogen. *Nature* **369**, 384–387 (1994).
18. Ashcroft, N. W. Pairing instabilities in dense hydrogen. *Phys. Rev. B* **41**, 10963–10971 (1990).
19. Belonoshko, A. B., Skorodumova, N. V., Rosengren, A. & Johansson, B. Melting and critical superheating. *Phys. Rev. B* **73**, 012201 (2006).
20. Finney, A. R. & Rodger, P. M. Applying the Z method to estimate temperatures of melting in structure II clathrate hydrates. *Phys. Chem. Chem. Phys.* **44**, 19979–19987 (2011).
21. Bader, R. Atoms in molecules: A quantum theory. Oxford Univ. Press, New York, 1990.
22. Henkelman, G., Arnaldsson, A. & Jonsson, H. A fast and robust algorithm for Bader decomposition of charge density. *Comp. Mat. Sci.* **36**, 354–360 (2006).
23. Baranowski, B. Charge transfer in hydrogen. *Physica B* **16**, 265 (1999).
24. Kresse, G. & Furthmüller, J. Efficiency of ab-initio total energy calculations for metals and semiconductors using a plane-wave basis set. *Comput. Mater. Sci.* **6**, 15–50 (1996).
25. Kresse, G. & Joubert, D. From ultrasoft pseudopotentials to the projector augmented-wave method. *Phys. Rev. B* **59**, 1758–1775 (1999).
26. Blöchl, P. E. Projector augmented-wave method. *Phys. Rev. B* **50**, 17953–17979 (1994).
27. Perdew, J. P., Burke, K. & Ernzerhof, M. Generalized Gradient Approximation Made Simple. *Phys. Rev. Lett.* **77**, 3865–3868 (1996).
28. Diatschenko, V. *et al.* Melting curves of molecular hydrogen and molecular deuterium under high pressures between 20 and 373 K. *Phys. Rev. B* **32**, 381–389 (1985).
29. Datchi, F., Loubeyre, P. & LeToullec, R. Extended and accurate determination of the melting curves of argon, helium, ice (H_2O), and hydrogen (H_2). *Phys. Rev. B* **61**, 6535 (2000).
30. Gregoryanz, E., Goncharov, A. F., Matsuishi, K., Mao, H.-K. & Hemley, R. J. Raman spectroscopy of hot dense hydrogen. *Phys. Rev. Lett.* **90**, 175701 (2003).
31. Deemyad, S. & Silvera, I. F. Melting line of hydrogen at high Pressures. *Phys. Rev. Lett.* **100**, 155701 (2008).
32. Eremets, M. I. & Trojan, I. A. Evidence of maximum in the melting curve of hydrogen at megabar pressures. *Pis'ma v Zh. Èksper. Teoret. Fiz.*, **89**:4, 198–203 (2009).

Acknowledgments

Author contributions

R.A. designed research; M.R. performed research; A.B.B., M.R., H.-K.M. and R.A. analyzed data; and A.B.B., M.R., H.-k.M. and R.A. wrote the paper.

Additional information